J Mol Model (2013) 19:705–714
DOI 10.1007/s00894-012-1594-x

ORIGINAL PAPER

Quantum chemistry studies of the catalysis mechanism differences between the two isoforms of glutamic acid decarboxylase

Chunling Wang · Rongxiu Zhu · Hainan Sun · Baiqing Li

Received: 30 May 2012 / Accepted: 30 August 2012 / Published online: 27 September 2012

Abstract The production of gamma-aminobutyric acid (GABA) is catalyzed by two isoforms of glutamic acid decarboxylase (GAD), using pyridoxal 5′-phosphate (PLP) as the cofactor. Between the two enzymes, GAD67 accounts for normal GABA requirement, while GAD65 stays inactive until emergent demand for GABA. Recent crystal structure findings revealed that the distinct conformation of a common catalytic loop of the enzymes may account for their different functions (Fenalti et al Nat Struct Mol Biol, 14:280-286, 2007). Enlightened by their inferences, we studied the underlying reaction mechanism of the two GAD isoforms using density functional theory (DFT). A rather complete reaction pathway is identified, including nine transition state (TS) structures and 14 intermediate (IM) structures. The rate limiting step occurs early during the reaction and involves a proton transfer. In the late stage, there are two pathways that involve C_4· and C_α protonation by Tyr or Lys. Our calculations show that the reaction barriers corroborate the conjecture made by Fenalti et al.

Keywords Density functional theory · Glutamic acid decarboxylase · Proton transfer · Pyridoxal 5′-phosphate · Transition state theory

Electronic supplementary material The online version of this article (doi:10.1007/s00894-012-1594-x) contains supplementary material, which is available to authorized users.

C. Wang · R. Zhu · H. Sun · B. Li (✉)
Institute of Theoretical Chemistry, School of Chemistry and Chemical Engineering, Key Laboratory of Colloid and Interface Chemistry (Ministry of Education), Shandong University, Jinan, Shandong 250100, People's Republic of China
e-mail: baiqingli@sdu.edu.cn

Introduction

Pyridoxal 5′-phosphate (PLP), the aldehyde form of vitamin B_6, is an indispensable cofactor of many enzymes, including those for transamination, decarboxylation, racemization, aldol cleavage and other reactions [1–5]. When no substrate is close by, its 4-formyl group is usually covalently bonded to the ε-amine group of a conserved lysine residue in the active site of the enzyme, forming an "internal" imine (also called Schiff base or azomethine). In the first step of the catalysis, PLP usually detaches from the lysine and binds the amine group of the substrate to form an "external" imine instead. The conjugation in the Schiff base-pyridine ring system extends from the α carbon of the amine (amino acid) to the pyridine nitrogen, leading to reduced electron density around the C_α atom due to the strong electron-withdrawing ability of the nitrogen atoms of the Schiff base and the pyridine (their electrophilicity can be even larger in protonated form). The bonds from the C_α to the hydrogen, the carboxyl, and the side chain are weakened, thus the "external" imine can lose an electrophile (e.g., H^+, CO_2 or the side chain), and transform into a carbanion intermediate (IM), also stabilized by the above π system. For this process, Dunathan suggested that the bond to be broken should align perpendicularly with the pyridine ring in the transition state (TS) of the reaction. This stereoelectronic hypothesis has been verified by subsequent studies and all PLP-catalyzed biochemical reactions are found to follow this mechanism in the early stages.

One important PLP-related reaction is the synthesis of gamma-aminobutyric acid (GABA), the chief inhibitory neurotransmitter, from glutamic acid, the chief excitatory neurotransmitter in mammals. This metabolic pathway, known as the GABA shunt, is catalyzed by glutamic acid decarboxylase (GAD). Distinct from most other biosynthetic processes, two isoforms of the enzyme, GAD67 and GAD65, are involved in catalyzing the same reaction.

Experimental findings revealed that GAD67 is responsible for the primary production of GABA, while GAD65 only responds when extra GABA is required. There are also two pathways for the catalysis of glutamic acid by PLP-GAD. The major one yields GABA, recovers PLP and keeps GAD active as a holoenzyme. Nevertheless the side reaction produces succinic semialdehyde (SSA) and pyridoxamine 5′-phosphate (PMP). PMP is unable to attach to the Lys on the enzyme, thus GAD becomes inactivated as an apoenzyme [6]. Experiments show that GAD65 catalyzes the side reaction at least 15 times faster than GAD67, therefore loses enzymatic activity rather quickly [7].

A recent paper provided structural explanations for the above functional difference [8]. The crystal structures show that the active sites of both isoforms include a lysine residue for attaching the PLP (Lys405 for GAD67, and Lys396 for GAD65), and are covered by a catalytic loop. The loop in GAD67 is more constrained and brings Tyr434 to the neighborhood of the C_α in PLP-Glu, thereby facilitating its protonation by Tyr434, the production of GABA and recovery of PLP. On the other hand, the loop in GAD65 is more mobile, and Tyr425 (aligned residue in GAD65 corresponding to Tyr434 in GAD67) is unable to protonate C_α efficiently, rather C_4· can be more readily protonated, possibly by Lys396 (which attaches PLP), leading to the side reaction and inactivation of the enzyme. The authors concluded that the different dynamic characteristics of the catalytic loop may be responsible for the distinct functions of the two GAD isoforms. Yet the structural resolution is insufficient for a complete mechanistic explanation [8]. The decarboxylation of Glu by PLP-GAD epitomizes the fundamental principle that many enzymes not only accelerate related reactions but also inhibit possible side reactions [3].

Enzyme reaction mechanisms have been attracting much attention due to its importance in understanding life processes and curing diseases. So far, the most well-acclaimed explanation is the *lock-and-key* model. Like gas phase reactions of small molecules, it can also be understood in terms of transition state theory (TST), with the transition barrier having a much bigger effect on enzymatic reaction rate than the transmission coefficient [9, 10]. A mere difference of 1.4 kcal mol^{-1} in the barrier height leads to a factor of 10 in the reaction rate. Much effort to entangle the enzyme catalysis mechanism has been devoted to probe the TS structures, yet up to now there are very few appropriate techniques, among which computational chemistry has been quite important [11].

The underlying principle of the computational chemistry approach is based on exploring the energy-geometry landscape of the reacting substrate, cofactor and enzyme for favorable reaction pathways that lead the reactants to the products. The routes can be constructed by identifying the intermediates and the transition states, or the stationary points on the energy-geometry map. The initial guesses of the transition states are usually based on chemical principles and previous findings, while those for the intermediates are usually calculated from related transition states using intrinsic reaction coordinate (IRC) method [12, 13]. The nature of the structures are confirmed by computing their vibrational frequencies, with the intermediates containing only positive ones (i.e., all eigenvalues of the Hessian matrix are positive), while the transition states including an imaginary one (i.e., one of the eigenvalues of the Hessian matrix is negative). Yet this approach suffers from two complexity issues due to the large size of enzymatic reaction systems, normally containing thousands or more of atoms. (1) The reaction landscape is extremely high-dimensional and prohibitively complicated. In principle, there can be numerous pathways connecting the reactants and the products, and so far it does not seem feasible to identify all of them. A customary way is to look for one or a few routes that conform to chemical sense and have reasonable activation barrier, allowing them to take place at enzyme operating temperature. (2) The large number of atoms, and therefore, the even larger number of electrons is far beyond the capability of even the most advanced electronic structure method and the state-of-the-art computers. Currently there are two primary approaches to avoid this problem. (1) The quantum chemistry method considers only a small part of the enzyme that contains the active site and the substrate, in the belief that most of the chemistry can be captured [14, 15]. The rest of the enzyme and the surrounding environment are totally left out in the calculations. (2) Instead, the hybrid quantum mechanics/molecular mechanics (QM/MM) method treats them with molecular mechanics (computationally much cheaper than quantum mechanics), therefore can partially recover their impact on the enzyme catalysis [16–18]. Yet QM/MM methods can be much more demanding on computer resources. So far both have had successes in uncovering enzymatic reaction mechanisms.

In this paper, we apply quantum chemistry method to study the reaction mechanism of a model GAD-Glu system and aim to provide more insight on the reaction mechanism of the GABA shunt in a more quantitative manner. A rather complete reaction pathway is constructed containing the TS and IM structures. The rest of the paper is organized as follows: after the introduction, the details of the model catalytic system and the computational methods are explained, next the results are presented, followed by discussion and conclusions.

Computational details

Starting from the reactants, a transition state structure is searched first, starting from initial structures constructed using previous knowledge and chemistry sense. The nature of transition state is confirmed if all the vibrational frequencies are positive except one being negative. Then internal reaction

coordinate calculations are performed to search for the intermediate structures in both the forward and backward directions, starting from the TS structure. This completes one reaction step, composed of an IM as reactant, a TS and an IM as product. This procedure is carried further until a rather complete reaction pathway is constructed that leads from the initial reactants to the final products. The free energy profile is also calculated to decide whether the reaction route has reasonable barrier heights. Usually the "product" IM structure of one reaction step does not coincide with the "reactant" IM of the next reaction step, but most of the transitions between them only involve single-bond rotations and rearrangement of intermolecular orientations, and do not break or form chemical bonds. These transitions are also expected to have small barriers, and are not determining factors of the reaction pathway, thus they are not studied.

All the calculations presented in this study are performed using the GAUSSIAN03 software package [19]. Geometry optimizations and vibrational frequencies are calculated with B3LYP functional [20, 21] using the 6–31 G(d,p) basis set to determine the stationary points. Single point calculations with the larger basis set B3LYP/6-311++G(d,p) are performed to obtain more accurate energies. Due to computational cost reasons, entropy and thermal corrections at 298.15 K are evaluated using the smaller basis set. To account for the influence from the solvent and the rest of the enzyme that is not included in the reaction model system, single point calculations with polarizable continuum model (PCM) are performed, with the dielectric constant ε chosen to be 4.0 to simulate protein environment.

Results and discussion

One reaction pathway with two branches in the late stage of the process is discovered and the related free energies are calculated. To make the explanation clearer, the overall action is divided into two stages, the formation of quinonoid and the protonation at C_{α} or $C_{4'}$.

Formation of quinonoid

During the first stage, glutamic acid (the substrate) replaces the lysine residue of the enzyme to form a quinonoid with the PLP cofactor, or the PLP converts from an inner aldimine with lysine to an external aldimine with glutamic acid. The model reaction system, denoted as R in Fig. 1, consists of a glutamic acid (to model the substrate), a PLP without the 6-phosphate group (to model the cofactor) and an ethylamine (to model lysine) connected through the C = N double bond. The PLP analogue and ethylamine are initially bonded together to reflect the fact that in PLP-aided biocatalysis, PLP is usually bonded to a lysine residue in the form of an internal imine in the absence of substrate, then detaches to form an external imine with the substrate to start the catalysis process. In the crystal structures obtained by Fenalti et al. a PLP molecule is found to be bonded to Lys405, and a GABA molecule is in the neighborhood. In the optimized structure, the N4-C2, C2-C3 and C2-N1 distances are 1.303Å, 1.463Å and 2.527Å respectively, and the N4-C2-C3-N5 dihedral angle is 22.83º (the number following the atomic symbol is from GAUSSIAN03 output).

The reduced model system is prescribed to save computational cost, but it does not compromise capturing essential chemistry. The truncated part of the substrate, the cofactor and the residues are believed to play non-deterministic roles, as do the intermolecular interactions from other residues in the vicinity of the reaction center. In fact biochemists often describe enzymatic reaction mechanisms using this type of simplified model, and in a similar manner as organic reactions, i.e., by the forming and breaking of covalent bonds, not intermolecular interactions.

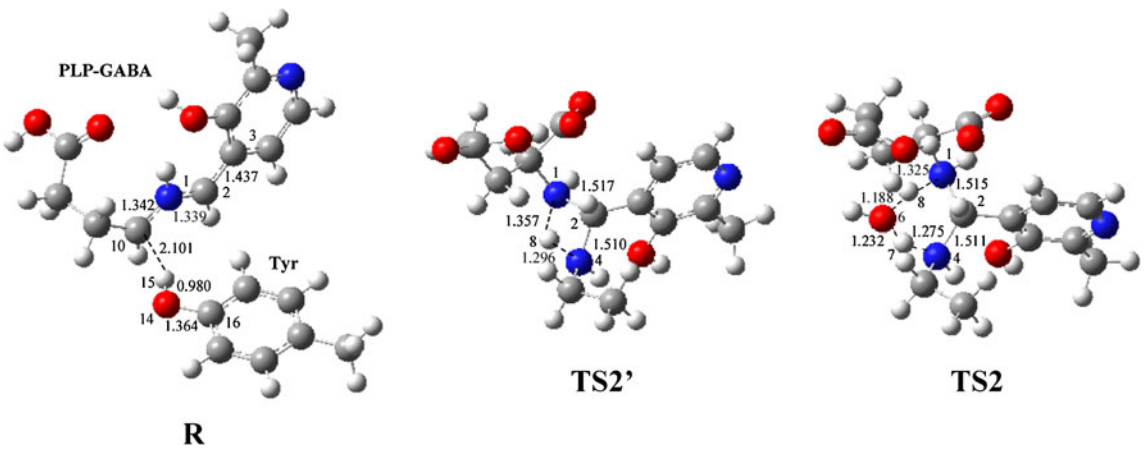

Fig. 1 Geometric configuration of the reactants R, and the transition states during the proton transfer step (without the aid of a water molecule, TS2', and with the aid of a water molecule, TS2)

The proposed reaction steps are summarized in Scheme 1, and the calculated free energy profile is shown in Fig. 2 for both in vacuo and in protein environment (ε=4.0). One should note that the structures in Fig. 1 only show the primary part of the model reaction system, yet the free energies in Fig. 2 include the terms from those moieties (H_2O, CO_2 and ethylamine) that have either detached or not yet attached to the main reaction molecules. This is reflected in Fig. 2 by arrows, for example, although the IM9 structure does not contain CO_2, the IM9 free energy in Fig. 2 does include the contribution from a detached CO_2 molecule. For example, the free energy of R also includes a detached H_2O and a Tyr/Lys analog (for the second stage of the reaction). It is used as the zero reference.

To start the biocatalysis, PLP needs to break away from lysine, and forms Schiff base with the glutamic acid. Based on this direction of reaction, the following reaction steps are conjectured and the transition state and intermediate structure are searched. The details are described as follows, (1) N4 (N_α of glutamic acid) attacks the $C_{4'}$, climbs over TS1 (the C2-N1 distance reduces from 2.527 Å in R to 1.969 Å in TS1) and forms a new C-N bond in IM1 (the C2-N1 bond length is 1.616 Å). The structures are presented in Supplementary materials. (2) H8 transfers from the glutamic acid to the ethylamine. Without a water molecule, the reaction has to go from IM1 to IM4 through TS2', with a rather high barrier of 23.9 kcal mol^{-1}, mostly because of the low stability of the N1-H8-C2-N4 four-membered ring as shown in Fig. 1. By adding a water molecule, which is abundant in enzymatic reaction systems (not explicitly drawn in Scheme 1), the proton transfer can proceed over a lower barrier passing TS2 (16.0 kcal mol^{-1}). The water molecule can assist the proton transfer because of the stability of the six-membered ring in TS2. Similar trend in 1,3-hydrogen-shift reactions due to water's participation has been observed in other computations [22]. The difference between IM1-IM2 and IM3-IM4 is the water molecule. IM4 proceeds further to IM5 through the rotation of the N1-C10 bond. The N1-C2 and C2-N4 bond lengths are 1.411 Å and 1.595 Å respectively. (3) Passing through TS3, the C-N bond between PLP and ethylamine breaks to form IM6, during which N1-C2 decreases from 1.348 Å to 1.300 Å, while C2-N4 increases from 1.861 Å to 2.770 Å. The reaction has a rather low barrier and can take place quite easily. Ethylamine further detaches from PLP-Glu and IM7 forms. The structures are presented in Supplementary materials.

Now PLP is no longer bonded to the enzyme (ethylamine representing lysine), it now forms a new Schiff base with the substrate (glutamic acid). At this stage, several reaction pathways can ensue: (1) loss of the carboxylic group as CO_2, i.e., decarboxylation; (2) loss of H_α, which normally advances

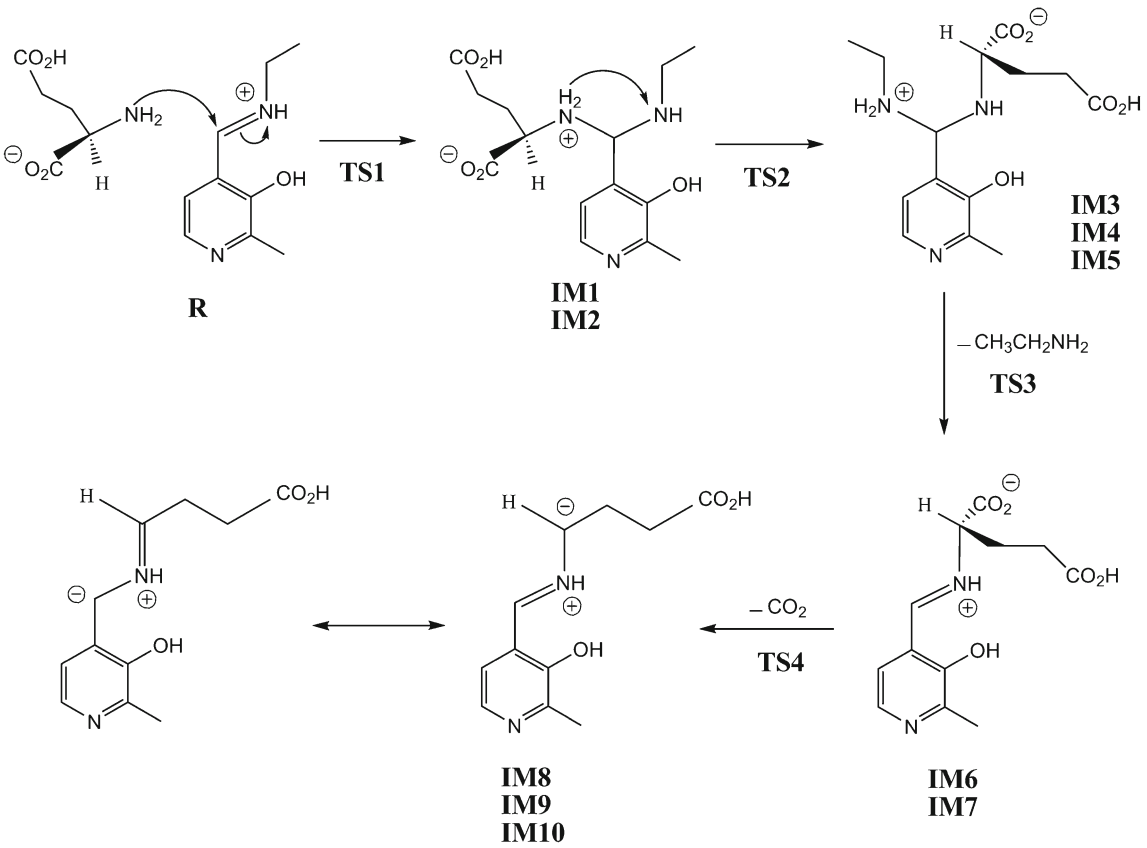

Scheme 1 The reaction steps leading to the formation of quinonoid

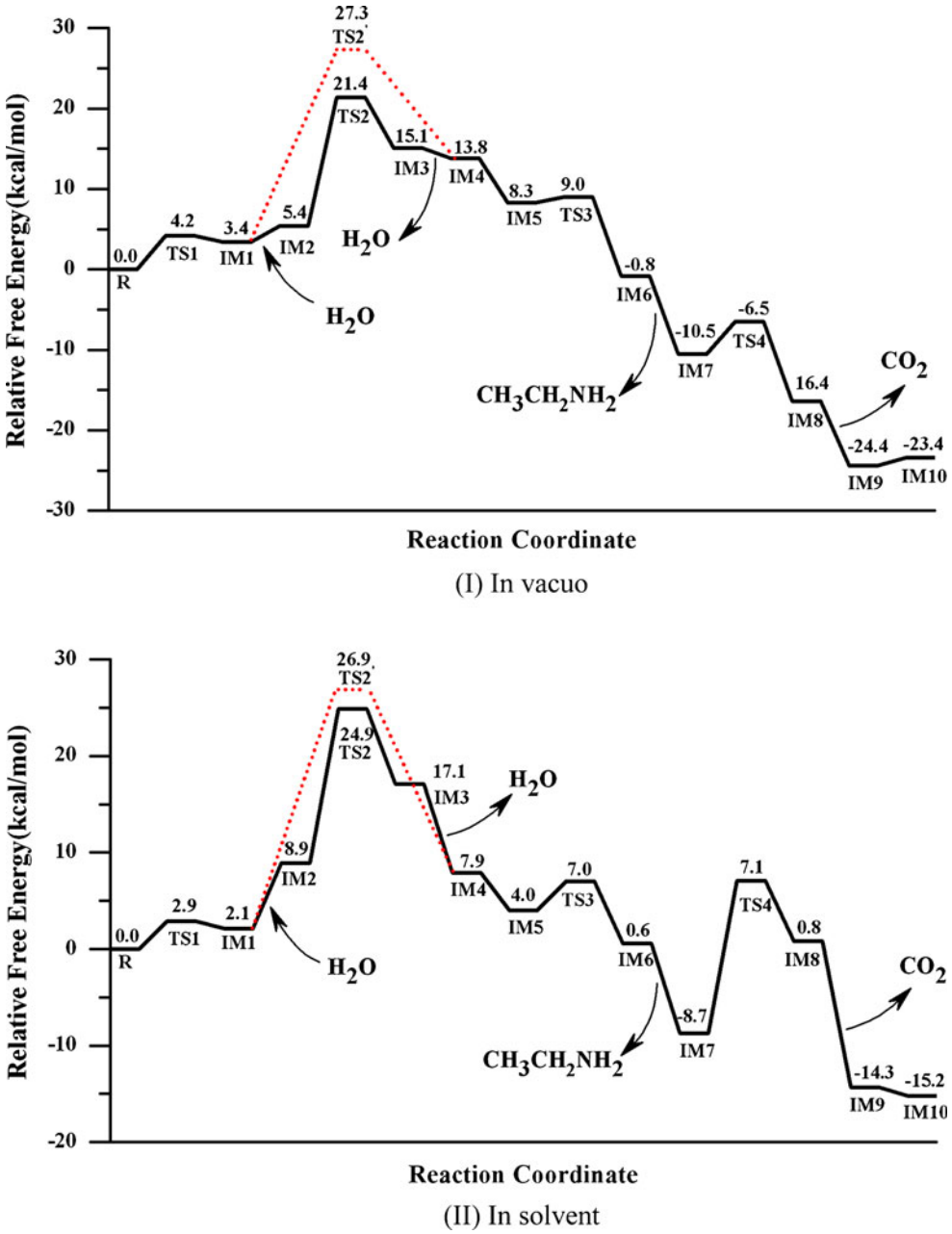

Fig. 2 Free energy profile of the reactions leading to the formation of the quinonoid: (I) in vacuo and (II) in protein environment

onto transamination, racemization and etc.; (3) cleavage of the bond between C_α and the side chain; (4) other processes. The multiple directions explain why PLP serves as the cofactor of a large number of enzymes. In current investigation, the carboxylic group in IM7 breaks away through TS4 to form IM8. As shown in Fig. 3, the C2-N1-10-11 dihedral angle is 80.4º in TS4 (57.6º in IM7), i.e., the carboxylic group is nearly perpendicular to the pyridine ring of PLP, in agreement with Dunathan's hypothesis. At the end of the first stage, IM8 detaches the CO_2 molecule to form IM9, a quinonoid, which further converts to IM10 through the rotation of the C10-C19 bond. The resonance structure of IM10 is presented in Scheme 1 because it is the starting configuration for the protonation reaction in the second stage. The single-bond rotation is expected to have relatively low barrier height, therefore the transition state is not searched.

As can be clearly observed in Fig. 2I for free energies in vacuo, the proton transfer from the glutamic acid to the ethylamine is the rate-limiting step, even with the aid from a water molecule. After including the effect from the protein surroundings using the PCM approach (ε=4.0), the energy is recalculated using the larger basis set with the structure optimized using the smaller basis in the gas phase. The entropy and the thermal correction still uses the in vacuo

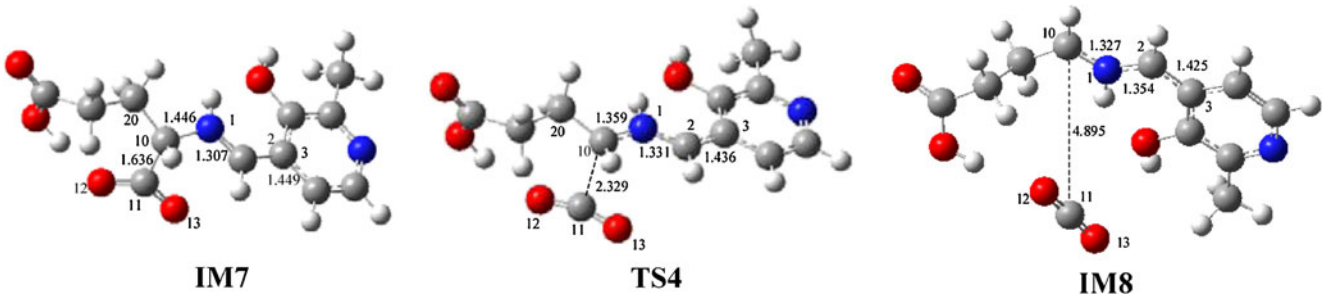

Fig. 3 Geometric configuration of the intermediates and the transition state of the decarboxylation step (IM7, TS4 and IM8)

data due to expensive computational cost. The reaction barrier profile reveals that the decarboxylation step (IM7-TS4) and the proton transfer step aided by a water molecule (IM2-TS2) have similar barrier heights (16 and 15.8 kcal mol^{-1}), and both appear to be the rate-limiting step. One should note that the barrier for the decarboxylation step is larger than the gas-phase results, possibly due to the decrease of polarity from IM7 to TS4.

Protonation at C_α or $C_{4'}$

The resonance structure of the PLP-Glu quinonoid in Scheme 1 reveals that both C_α and $C_{4'}$ have some carbanion characteristic (this can also be observed through charge population analysis using Gaussian software package) and are good "candidates" for attaching protons. The extended π electron system helps to stabilize the negative charge, and is

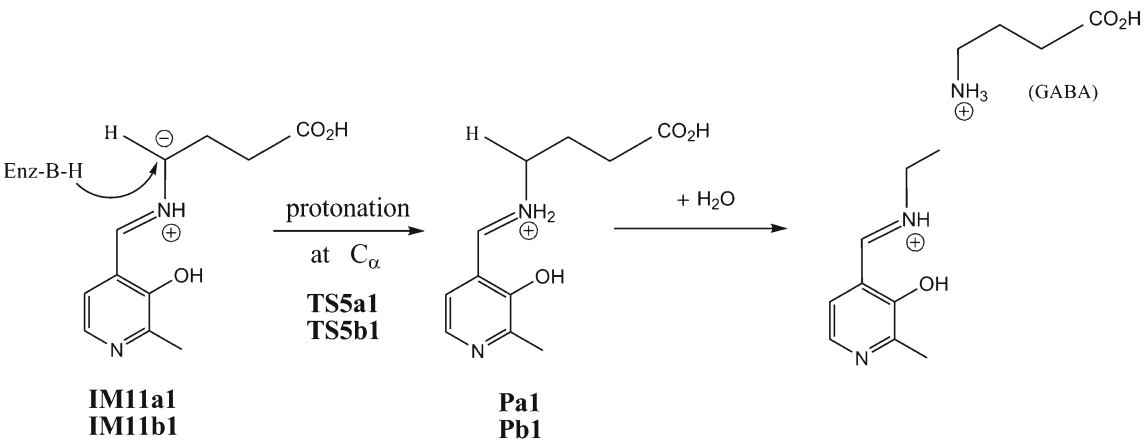

Pathway 1 Protonation at C_α and subsequent hydrolysis

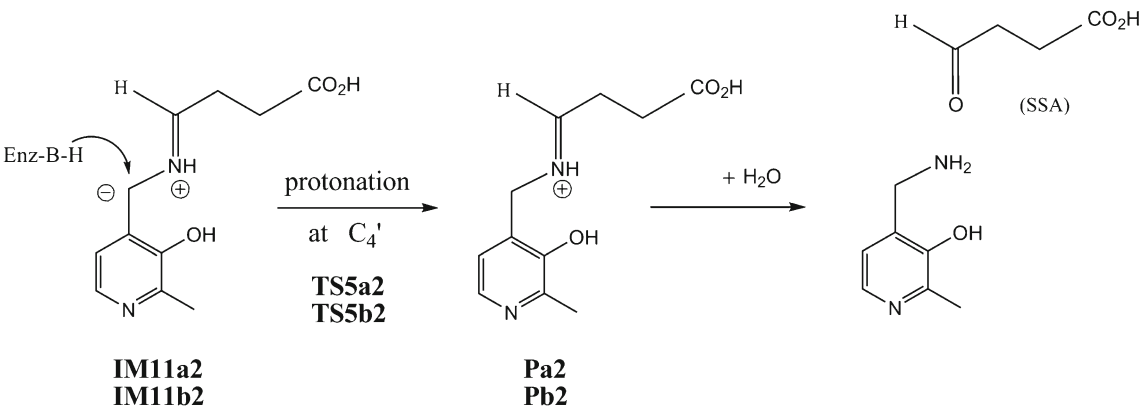

Pathway 2 Protonation of $C_{4'}$ and subsequent hydrolysis

Scheme 2 Protonation reaction of PLP-Glu of C_α (*pathway 1*) and $C_{4'}$ (*pathway 2*) and subsequent hydrolysis

often referred to as an "electron sink". The protonation of either C_α or $C_{4'}$, as illustrated in Scheme 2 for the reactions in the second stage, leads to different Schiff bases. The Schiff bases can readily undergo hydrolysis and yield an aldehyde and an amine, and are not studied here. In pathway 1, C_α is protonated, GABA is produced and PLP is recovered and can again function as the cofactor, while in pathway 2, $C_{4'}$ gets the proton and SSA forms, PLP converts to the amine form, PMP, which is unable to combine with the lysine residue on the enzyme, thus the enzyme is converted to the inactive apo-form.

The crystal structure studies by Fenalti et al. disclosed that the active sites of both GAD67 and GAD65 are covered by a catalytic loop [8]. The GAD67 loop is more constrained and brings Tyr434 to the neighborhood of the C_α in PLP-Glu, thereby facilitates its protonation by Tyr434, the production of GABA and the recovery of PLP. In addition, the loop also hinders the hydrolysis product PLP from moving away from the active site, therefore fosters its reuse in the enzymatic cycle. Yet the loop in GAD65 is more mobile, and Tyr425 (aligned residue corresponding to Tyr434 in GAD67) is unable to protonate C_α efficiently, rather $C_{4'}$ can be more readily protonated, possibly by Lys396 close

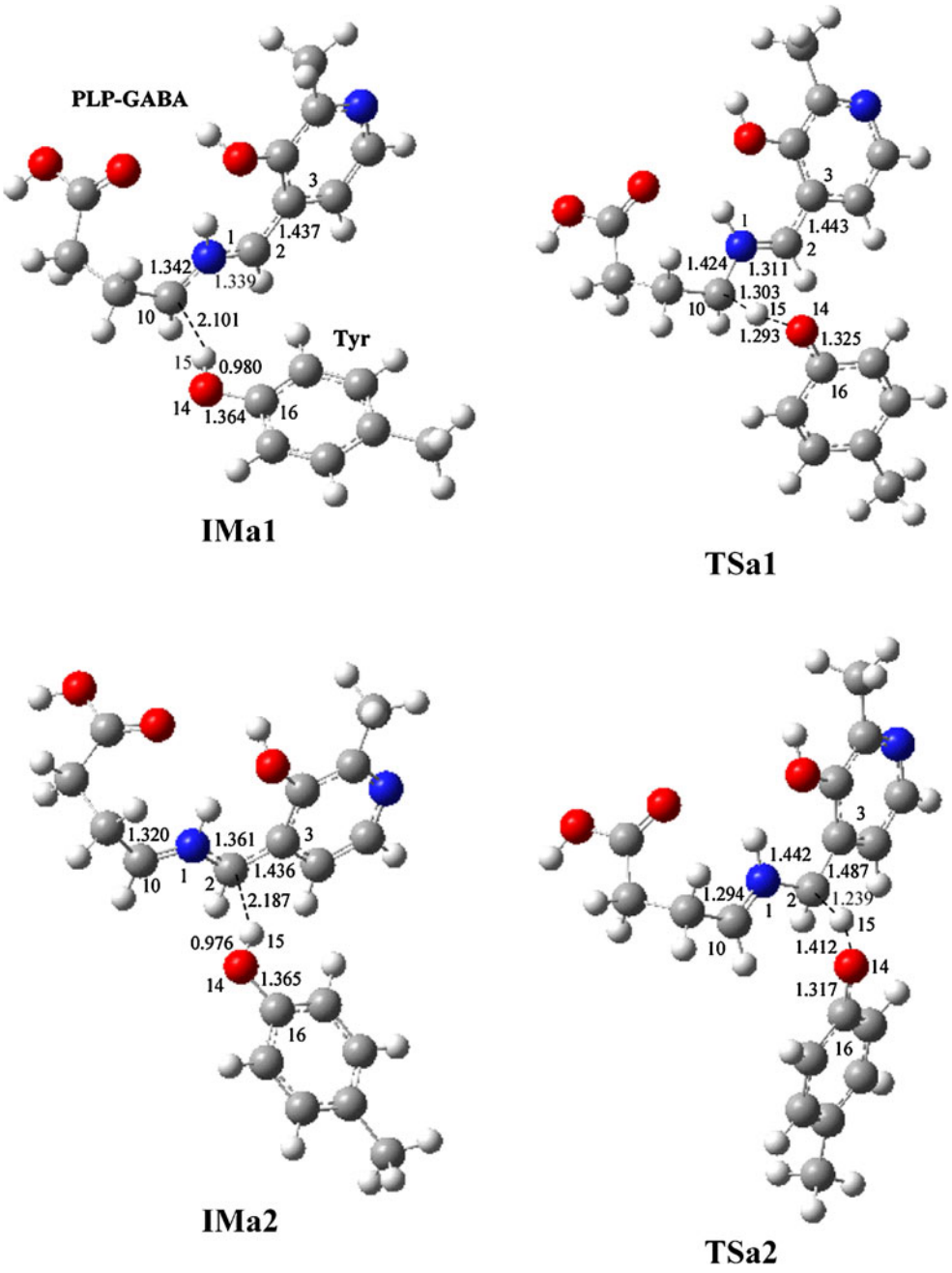

Fig. 4 Geometric configuration of the intermediates, transition states and products during the protonation of (1) C_α and (2) $C_{4'}$ by Tyr

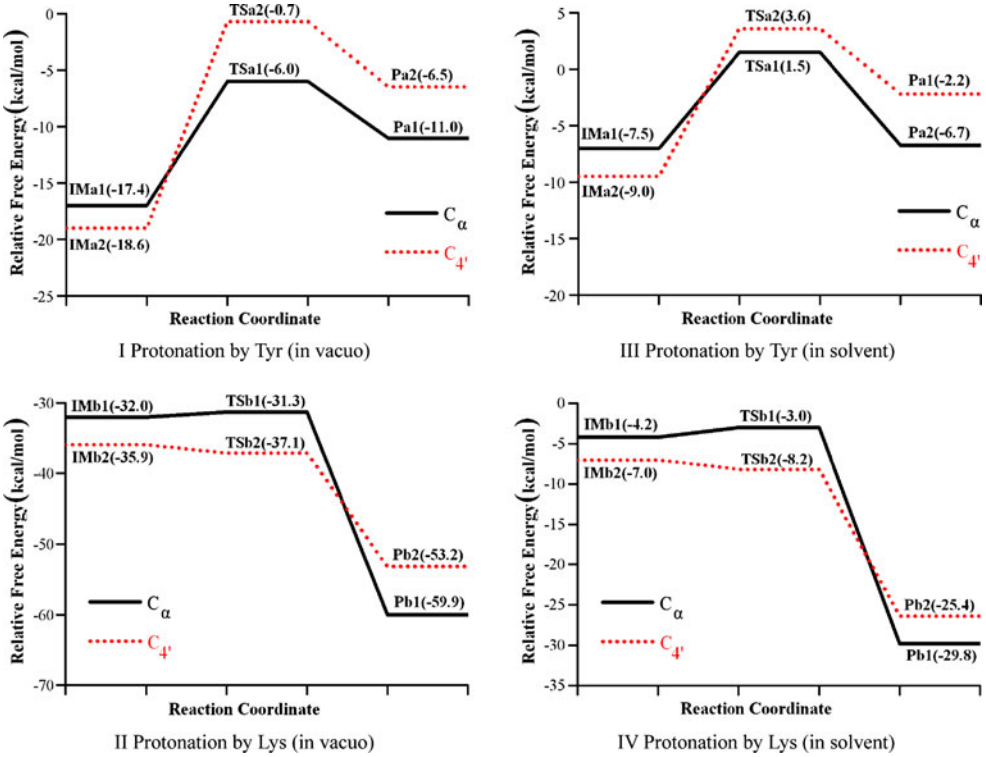

Fig. 5 Free energy profile of the protonation step of (1) C_{α} and (2) $C_{4'}$ by (**a**) Tyr and (**b**) by Lys (I and II: in vacuo, III and IV: in protein environment)

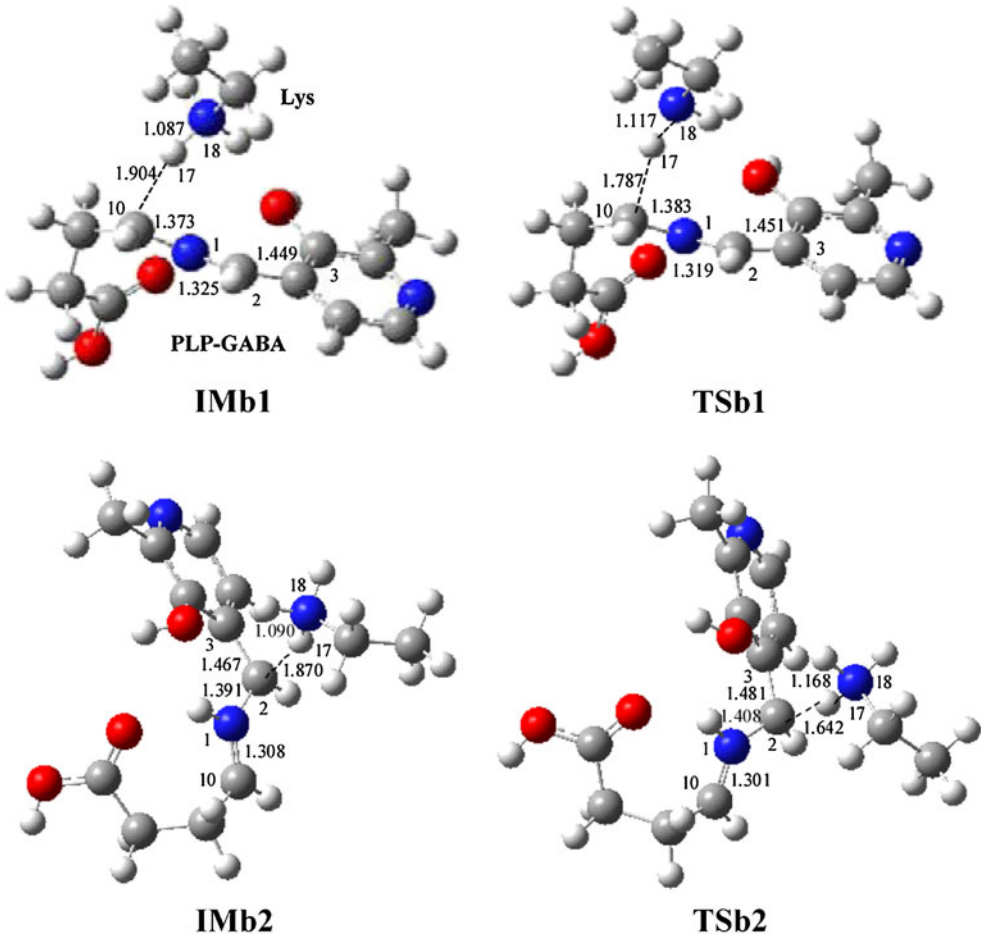

Fig. 6 Geometric configuration of the intermediates and transition states during the protonation of (1) C_{α} and (2) $C_{4'}$ by Lys

by, leading to the side reaction and inactivation of the enzyme. Furthermore the loop allows PMP to move relatively easily away from the active site. The authors proposed this as the underlying reason for the distinct functions of the two GADs. They also pointed out that the structural resolution is insufficient for a complete mechanistic explanation.

Based on their conjectures, we studied the reaction pathways using either Tyr (a) or Lys (b) as the protonation agent at either C_α or C_4·. We are able to identify the intermediate and the transition state structures of all four possible reaction routes. For C_α protonation by Tyr as shown in Fig. 4, C10(C_α)-H15 and O14-H15 changes from 2.101 Å and 0.980 Å in IMa1 to 1.303 Å and 1.293 Å in TSa1, while for C_4· protonation by Tyr, C2(C_4·)-H15 and O14-H15 changes from 2.187 Å and 0.976 Å in IMa2 to 1.412 Å and 1.239 Å in TSa2. Both involve the proton transfer from oxygen to carbon and the formation of a C-H bond and the dissociation of an O-H bond. As shown in Figs. 5I, the barrier height for C_α protonation is 11.4 kcal mol^{-1}, while that of C_4· protonation is 17.9 kcal mol^{-1}, thus C_α has a stronger tendency to get the proton from Tyr than C_4·.

For C_α protonation by Lys as shown in Fig. 6, C10(C_α)-H15 and N18-H15 changes from 1.904 Å and 1.087 Å in IMb1 to 1.787 Å and 1.117 Å in TSb1, while for C_4· protonation by Lys, C2(C_4·)-H15 and N18-H15 changes from 1.870 Å and 1.090 Å in IMb2 to 1.642 Å and 1.168 Å in TSb2. Both show the proton transfer from nitrogen to carbon and the formation of a C-H bond and the dissociation of an N-H bond.

Figure 5II shows that TSb2 is 1.2 kcal mol^{-1} lower in free energy than IMb2, yet TSb2 is 0.5 kcal mol^{-1} higher in electronic energy than IMb2. A similar trend has been observed elsewhere, and the harmonic approximation in calculating vibrational frequency has been suspected to be the cause [23]. C_α protonation has a barrier height of 0.7 kcal mol^{-1}, therefore kinetically Lys tends to give the proton to C_4· rather than C_α. What's more, the C_α pathway recovers the PLP, while the C_4· pathway is irreversible, and PLP can be fast depleted, leading to the enzyme's deactivation.

Including solvent effect yields similar trend in the free energy profiles, as displayed Fig. 5III and IV. One should also note that although the transition state of C_α protonation (pathway 1) by Tyr or Lys has a larger conjugation system than the corresponding one of C_4· protonation (pathway 2), its free energy is not necessarily lower (TSa1 < TSa2, TSb1 > TSb2). The structures of the intermediates and transition states that are not shown in the main text are provided in Fig. S1 of Supplementary materials.

Conclusions

Enlightened by recent crystallography results and conjectures based on them [8], we performed a computational quantum chemistry study on the distinct catalytic mechanisms of the two isoforms of glutamic acid decarboxylase. The model enzyme reaction system consists of a pyridoxal 5′-phosphate analogue (the cofactor), a glutamic acid (the substrate) and a lysine and a tyrosine/lysine residue (the enzyme). A reaction pathway is identified, containing nine transition state structures and 14 intermediate structures. The reaction barriers indicate that the pathway is plausible. The rate limiting step occurs early during the reaction and involves a proton transfer. Water can help lower the reaction barrier of this reaction. To test the mechanism proposed by Fenalti et al., we investigated the protonation of C_4· and C_α on the PLP by Tyr or Lys in the late stage of the reaction. The free energy barriers indicate that Tyr favors protonating C_α, while Lys favors protonating C_4·. This coincides with the conjecture proposed by Fenalti et al. that Tyr434 protonates C_α in GAD67, while Lys396 protonates C_4· in GAD65 based on spatial proximity from crystal structure findings. Our studies reflect two determining factors for chemical reactions to occur: geometry and free energy.

Acknowledgments We would like to thank the support from National Natural Science Foundation of China (Grant No. 21073108), Ministry of Education of China (Grant No. 20090131120020) and Independent Innovation Foundation of Shandong University (Grant No. 2012TS006).

References

1. Metzler DE (2001) Biochemistry: the chemical reactions of living cells, 2nd ed, Vol 1. Academic, San Diego
2. Zempleni J, Rucker RB, Suttie JW, McCormick DB (2007) Handbook of vitamins, 4th ed. CRC, New York
3. Christen P, Mehta PK (2001) Chem Rec 1:436–447
4. Dunathan HC (1966) Proc Natl Acad Sci USA 55:712–716
5. Eliot AC, Kirsch JF (2004) Annu Rev Biochem 73:383–415
6. Porter TG, Spink DC, Martin SB, Martin DL (1985) Biochem J 231:705–712
7. Battaglioli G, Liu H, Martin DL (2003) J Neurochem 86:879–887
8. Fenalti G, Law RHP, Buckle AM, Langendorf C, Tuck K, Rosado CJ, Faux NG, Mahmood K, Hampe CS, Banga JP, Wilce M, Schmidberger J, Rossjohn J, El-Kabbani O, Pike RN, Smith AI, Mackay IR, Rowley MJ, Whisstock JC (2007) Nat Struct Mol Biol 14:280–286
9. Benkovic SJ, Hammes-Schiffer S (2003) Science 301:1196–1202
10. Garcia-Viloca M, Gao J, Karplus M, Truhlar DG (2011) Science 303:186–195
11. Schramm VL (2005) Arch Biochem Biophys 433:13–26
12. Gonzalez C, Schlegel HB (1989) J Chem Phys 90:2154–2161
13. Gonzalez C, Schlegel HB (1990) J Phys Chem 94:5523–5527
14. Himo F (2005) Theor Chem Acc 116:232–240
15. Siegbahn PEM, Himo F (2011) Wiley Interdiscip Rev Comput Mol Sci 1:323–336
16. Warshel A, Levitt M (1976) J Mol Biol 103:227–249
17. Field MJ, Bash PA, Karplus MJ (1990) J Comput Chem 11:700–733
18. Senn HM, Thiel W (2009) Angew Chem Int Ed 48:1198–1229

19. Frisch MJ, Trucks GW, Schlegel HB, Scuseria GE, Robb MA, Cheeseman JR, Montgomery JA Jr, Vreven T, Kudin KN, Burant JC, Millam JM, Iyengar SS, Tomasi J, Barone V, Mennucci B, Cossi M, Scalmani G, Rega N, Petersson GA, Nakatsuji H, Hada M, Ehara M, Toyota K, Fukuda R, Hasegawa J, Ishida M, Nakajima T, Honda Y, Kitao O, Nakai H, Klene M, Li X, Knox JE, Hratchian HP, Cross JB, Bakken V, Adamo C, Jaramillo J, Gomperts R, Stratmann RE, Yazyev O, Austin AJ, Cammi R, Pomelli C, Ochterski JW, Ayala PY, Morokuma K, Voth GA, Salvador P, Dannenberg JJ, Zakrzewski VG, Dapprich S, Daniels AD, Strain MC, Farkas O, Malick DK, Rabuck AD, Raghavachari K, Foresman JB, Ortiz JV, Cui Q, Baboul AG, Clifford S, Cioslowski J, Stefanov BB, Liu G, Liashenko A, Piskorz P, Komaromi I, Martin RL, Fox DJ, Keith T, Al-Laham MA, Peng CY, Nanayakkara A, Frisch MJ, Trucks GW, Schlegel HB, Scuseria GE, Robb MA, Cheeseman JR, Montgomery JA Jr, Vreven T, Kudin KN, Burant JC, Millam JM, Iyengar SS, Tomasi J, Barone V, Mennucci B, Cossi M, Scalmani G, Rega N, Petersson GA, Nakatsuji H, Hada M, Ehara M, Toyota K, Fukuda R, Hasegawa J, Ishida M, Nakajima T, Honda Y, Kitao O, Nakai H, Klene M, Li X, Knox JE, Hratchian HP, Cross JB, Bakken V, Adamo C, Jaramillo J, Gomperts R, Stratmann RE, Yazyev O, Austin AJ, Cammi R, Pomelli C, Ochterski JW, Ayala PY, Morokuma K, Voth GA, Salvador P, Dannenberg JJ, Zakrzewski VG, Dapprich S, Daniels AD, Strain MC, Farkas O, Malick DK, Rabuck AD, Raghavachari K, Foresman JB, Ortiz JV, Cui Q, Baboul AG, Clifford S, Cioslowski J, Stefanov BB, Liu G, Liashenko A, Piskorz P, Komaromi I, Martin RL, Fox DJ, Keith T, Al-Laham MA, Peng CY, Nanayakkara A, Challacombe M, Gill PMW, Johnson B, Chen W, Wong MW, Gonzalez C, Pople JA (2004) Gaussian03. Gaussian Inc, Wallingford
20. Lee C, Yang W, Parr RG (1988) Phys Rev B 37:785–789
21. Becke AD (1993) J Chem Phys 98:5648–5652
22. Song G, Su Y, Periana RA, Crabtree RH, Han K, Zhang H, Li X (2010) Angew Chem Int Ed 49:912–917
23. Yang X, Hall MB (2010) J Am Chem Soc 132:120–130